

# Exact solutions for thermomagnetized unsteady non-singularized Jeffrey fluid: Effects of ramped velocity, concentration with Newtonian heating

Aziz-Ur-Rehman<sup>a</sup>, Muhammad Bilal Riaz<sup>a,b,c</sup>, Jan Awrejcewicz<sup>c</sup>, Dumitru Baleanu<sup>d,e,f,\*</sup>

<sup>a</sup> Department of Mathematics, University of Management and Technology Lahore, Pakistan

<sup>b</sup> Institute for Groundwater Studies (IGS), University of the Free State, South Africa

<sup>c</sup> Department of Automation, Biomechanics and Mechatronics, Lodz University of Technology, 1/15 Stefanowskiego St., 90-924 Lodz, Poland

<sup>d</sup> Department of Mathematics, Cankaya University, 06530 Ankara, Turkey

<sup>e</sup> Institute of Space Sciences, Magurele, 077125 Bucharest, Romania

<sup>f</sup> Department of Medical Research, China Medical University Hospital, China Medical University, Taichung, Taiwan

## ARTICLE INFO

### Keywords:

Newtonian heating  
Laplace transform  
Memory effect  
Jeffrey fluid  
Ramped conditions  
Time fractional differential operator

## ABSTRACT

The classical calculus due to the fact that it assumed as the instant rate of change of the output, when the input level changes. Therefore it is not able to include the previous state of the system called memory effect. But in the Fractional Calculus (FC), the rate of change is affected by all points of the considered interval, so it is able to incorporate the previous history/memory effects of any system. Due to the importance of this effect we used the modern concept of the Caputo-Fabrizio fractional derivative on the considered Jeffrey fluid model. In this paper the effect of Newtonian heating, concentration and velocity on unsteady MHD free convective flow of Jeffrey fluid over long vertical an infinite ramped wall nested in porous material are discussed. Exact analytical solutions are derived via Laplace transformation technique for principal equations of energy, concentration and ramped velocity. The prime features of various coherent parameters are deliberated and illuminated with the aid of plotted graphs. A comparative study to show the significance of fractional order model with an integer order model is accomplished. The fractional order model is found to be the best choice for explaining the memory effect of the considered problem. It is identified that temperature distribution, concentration and ramped velocity profiles for fractional model are converges to an ordinary model when fractional parameter tends to integer order, which shows that fractional model is more appropriate to explicate experimental results.

## Introduction

Non-Newtonian fluids flow not only exists in nature, for instance, avalanches and mud slides, but also in modern technologies and many industrial sectors due to their important applied utilities such as biological materials (blood), pharmaceutical, chemicals (polymers, paints, plastics), foodstuffs (yogurt, ketchup, honey) and personal care items (creams, toothpastes, shampoo, gel), etc. In the current years, non-Newtonian fluids natural convection flow effected by MHD forces have applications in energy generators, power elevators, polymer fabrication, aerodynamic heating, accelerators and the refinement of inorganic oil and hydrogeologists investigated the fluid convective flows which is in porous constituents in order to prediction their rejoinders in numerous types of artificial lake [1–3]. The purpose of fluids which is non-Newtonian expecting the performances cannot be abstracted by

assuming a one single model. Flow equations becomes more complex due to shear rate and shear stress non-linear relation as compared to the Navier–Stokes equation can describe, developes and explain their order [4,5]. However, in the literature scant models are present to forecast the structures of such types of fluids. The main three classes of such types of models include rate type, differential and Integral models. Rate type models for research point of view are more applicable as they expect both elastic effects and memory. Among the numerous non-Newtonian fluid models, Jeffrey model is one of such non-Newtonian fluid models that attract several researchers due to its deliberation as a physiological better fluid model [6–8]. Also, this model is known as a generalisation of the recurrently used Newtonian model due to the fact that its fundamental equation can be concentrated Newtonian model's as a special case of such model. Moreover, the Jeffrey model described the characteristic of memory time scale and stress relaxation property, but usual

\* Corresponding author.

E-mail address: [dumitru.baleanu@gmail.com](mailto:dumitru.baleanu@gmail.com) (D. Baleanu).

<https://doi.org/10.1016/j.rinp.2021.104367>

Received 8 April 2021; Received in revised form 18 May 2021; Accepted 19 May 2021

Available online 1 June 2021

2211-3797/© 2021 Published by Elsevier B.V. This is an open access article under the CC BY-NC-ND license (<http://creativecommons.org/licenses/by-nc-nd/4.0/>).

viscous fluid model cannot describe this property.

Many numerical and analytical investigations on Jeffrey fluid have been carried out. Among them, Hayat et. al. [9] was explored time reliant mixed convection flow of Jeffrey fluid over a extending surface in the existence of heat discharge. For the convective movement of Jeffrey fluid a numerical analysis of energy transfer and entropy generation was performed by Dalir et. al. [10]. A model identified by Abo-Elkhair and Mekheimer [11] for blood passing in the vessels by examining the genetic and corporal characteristics of Jeffrey MHD flow in constricting and intensifying walls. Abro et. al. [12] examined the comprehensive oscillatory MHD Jeffrey fluid circulation to examine the impact of thermal, nonlinear heat discharge on energy transfer.

All aforementioned studies which have countless suitable consequences, but only combine either constant or uniform conditions at end points. According to our valuable information, for Jeffrey fluid there does not exist a single paper or article in the published literature which have complete knowledge regarding to analyzed the influence of ramped conditions on velocity profile, energy and concentration at the identical time. Furthermore, researchers conducted computational studies and physical experiments reviewed in chemical industry and in the medical fields use of these conditions has several applications. For instance, detecting cardiovascular infections involve ergometers, this function base on ramped velocity conditions [13]. Diagnostic analysis, check working of a blood circulation system and influential treatments contain applications of velocity with ramped conditions applied. However, Belin and Myers et.al. [14] and Bruce [15] applied velocity with ramped conditions to assess the boundaries of consider the workout tolerance, thermal therapy is used to analyze the cancer patient which is also based on such type of conditions was studied by Kundu [16].

Credit should be given to Malhotra, Hayday and Schetz [17–19] for presenting the temperature under ramped conditions. Impacts of ramped temperature on viscous convective fluids flow was analyzed by Chandran et. al. [20]. Also, Seth enhanced this work and studied natural, moving plates in vertical form to discover the influence of ramped wall temperature on physical such phenomena like Hall current, chemical sensitivities, thermal diffusivity and immersion in porous material [21–25]. A study was accomplished by Narahari et al. [26] fluid flow for an infinite plate hanged vertically with a heated wall. Behaviour of MHD Jeffrey fluid flow was studied by Khan's [27], which was prolonged by Zin et. al. [28] and obtained the precise solution for natural convective motion of Jeffrey MHD fluid in the presence of ramped temperature conditions.

It is observed that there is a lack of articles in the literature describes flows with concentration, temperature and velocity under ramped conditions, regardless of the appreciated practical insinuations. Ramped conditions used at similar time was firstly presented by Ahmed and Dutta [29] to examine the time dependent natural convection motion of a Newtonian type fluid in porous medium past an impulsively happened upright plate which is infinite with ramped velocity, ramped wall temperature and concentration. Maqbool et. al. [30] has studied the effects of ramped conditions on unsteady free convection of Jeffrey fluid flow in a porous material. Also, Mazhar et. al. [31] investigated the impact of applied ramped conditions simultaneously on Oldroyd-B fluid.

The non-integer differential operators Caputo-Fabrizio is a fractional operator which transformed the ordinary model to generalized model. In context with fractional derivatives, Abro [32] investigated a comparative study of thermo-diffusion impacts on natural convection flow between fractional and non-fractional differential operator and also find solution via Laplace transformation and Fourier sine transform. In the published literature various types of fractional operators like Caputo (Power law), Caputo-Fabrizio (exponential law), Atangana-Baleanu (Mittage-Leffler law) and several others are discussed [33–37]. Riaz et al. [38] studied temprature for non-singular kernel convective flow with ramped conditions. Further, the same author Riaz et al. [39] highlighted the heat effect on MHD Maxwell fluid by using non-local and local operators. Some other associated references dealing with fractional

maxwell MHD fluid movement, heat emission or fractional second grade fluid are give in [40–42, 47–49]. Recently, Talha Anwar et. al. [43] studied MHD free convective movement of Jeffrey fluid under the influence of Newtonian heating with ramped conditions on velocity via Caputo-Fabrizio approach. To obtained the solution they applied Stethfest's and Zakian's numerical Algorithm but not find the exact solution. According to our best knowledge not a single result is presented in the published literature which have exact solution with Caputo-Fabrizio time fractional operator. Based on the aforementioned literature, this work intents to use Caputo-Fabrizio time fractional operator on MHD free convective stream of Jeffrey fluid and compared with the derived solutions by Talha Anwar et al. [43].

In the present work, keeping the above mentioned results in view, the sole motive of present research is analyzed the impacts of different system parameters on ramped velocity, concentration with Newtonian heating applied on unsteady convective motion of MHD Jeffrey fluid over an infinite steep plate which is fixed in porous medium. Techniques of Laplace transformation method, as in the literature, is utilized to get analytical solution via Caputo-Fabrizio time fractional operator for ramped wall velocity with Newtonian heating and concentration from dimensionless governing equations. To analyzed the physical significance of the considered problem, estimated the values of ramped wall velocity with Newtonian heating and concentration, with the aid of graphically illustrations for several values of copious parameters like  $P_r$ , the relaxation time parameter  $\lambda_1$ , the retardation time parameter  $\lambda_2$ , Magnetic number  $M$ , dimensionless time  $t$ ,  $S_c$ ,  $G_m$ ,  $G_r$  and  $\alpha$ . Furthermore, some results found in the literature as limiting cases were extracted from our current findings.

## Mathematical model

The equations which illustrate unsteady MHD natural convective motion of Jeffrey fluid over a vertical limitless ramped wall is written as:

$$\nabla \cdot \nabla = 0, \nabla \cdot T + \rho g + \mathbb{J} = \rho \left[ (\nabla \cdot \nabla) \nabla + \frac{\partial \nabla}{\partial t} \right], \quad \mathbb{J} = J \times M. \quad (1)$$

where  $\nabla$ ,  $\rho$ ,  $J$  and  $M$  are represented by velocity distribution, density, electric density and total magnetic field (imposed and induced) respectively. The basic equations for Jeffrey fluid in which cauchy stress and extra stress tensor are represented by  $T$  and  $\mathbb{S}$  respectively, is written as

$$T = -pI + \mathbb{S}, (1 + \lambda_1) \mathbb{S} = \mu \left[ \mathbb{A} + \lambda_2 \left( \frac{\partial \mathbb{A}}{\partial t} + (\nabla \cdot \nabla) \mathbb{A} \right) \right], \mathbb{A} = (\nabla \nabla)^T + (\nabla \nabla), \quad (2)$$

In the above equations,  $\lambda_1$ ,  $\mu$ ,  $\lambda_2$ ,  $-pI$  and  $\mathbb{A}$  are denoted by ratio of relaxation to retrdation time, dynamic viscosety, retardation time, tensor's indeterminate part and Rivlin-Ericksen tensor respectively. Furthermore, from Eq. (2) we get the expression for classical viscous Newtonian fluid when  $\lambda_1 = \lambda_2 = 0$ . Also, Maxwell Equations for magnetic and electric field are defined in the following way

$$\Delta \cdot M = 0, \quad \Delta \times M = \mu_m J, \quad \Delta \times E = -\frac{\partial M}{\partial t}. \quad (3)$$

where  $J$ ,  $M$  and  $\mu_m$  are denoted by electric field, magnetic field and magnetic permeability respectively. Furthermore,  $M = M_0 + M_1$  in which  $M_0$  is denoted by imposed magnatic field and  $M_1$  is induced magnatic field which is not considered in this situation. Assume that the fluid flow is one dimensional and unidirectional,  $\nabla$  and  $\mathbb{S}$  are velocity and shear stress in the shape of

$$\nabla = w(y, t) \hat{i} \quad \text{and} \quad \mathbb{S} = \mathbb{S}(y, t). \quad (4)$$

where  $w$  is denoted by x-component of the velocity  $\nabla$ . Initially, Jeffrey fluid is at rest, at time  $t = 0$ , with adjacent wall having constant concentration  $C_\infty$  and temperature  $T_\infty$ . When  $t \leq t_0$  the velocity of the wall

becomes  $w_0 \frac{t}{t_0}$ , but for time  $t > t_0$  the wall maintained the uniform velocity  $w_0$ . The stress field which satisfy  $\mathbb{S}(y, 0) = 0$ , gives the following results  $\mathbb{S}_{xx} = 0, \mathbb{S}_{yy} = 0, \mathbb{S}_{zz} = 0, \mathbb{S}_{xz} = 0, \mathbb{S}_{yz} = 0, \mathbb{S}_{zx} = 0, \mathbb{S}_{zy} = 0$  and

$$(1 + \lambda_1)\mathbb{S}_{xy} = \mu \left[ 1 + \lambda_2 \frac{\partial}{\partial t} \right] \frac{\partial w}{\partial y}. \tag{5}$$

where  $\mathbb{S}_{xy}$  represent the non-trivial tangential stress. Moreover, to analyze the energy transfer, assume that the impression of thermic radiation in normal direction along the wall suppressed to Newtonian heating in first figure is described. The principal governing equations for Jeffrey fluid, energy, shear stress and concentration can be expressed subject to the Boussinesq's approximation and Rosseland approximation [44–46] are given as:

$$\frac{\partial w(y, \bar{t})}{\partial \bar{t}} = \frac{\nu}{1 + \lambda_1} \left( 1 + \lambda_2 \frac{\partial}{\partial \bar{t}} \right) \frac{\partial^2 w(y, \bar{t})}{\partial y^2} + g\beta_T (T(y, \bar{t}) - T_\infty) + g\beta_C (C(y, \bar{t}) - C_\infty) - \frac{\sigma\beta_0^2}{\rho} w(y, \bar{t}), \tag{6}$$

$$\frac{\partial T(y, \bar{t})}{\partial \bar{t}} = \frac{k}{\rho c_p} \left( 1 + \frac{16\sigma_1 T_\infty^3}{3kK_1} \right) \frac{\partial^2 T(y, \bar{t})}{\partial y^2}, \tag{7}$$

$$(1 + \lambda_1)\mathbb{S}(y, \bar{t}) = \mu \left( 1 + \lambda_2 \frac{\partial}{\partial \bar{t}} \right) \frac{\partial w(y, \bar{t})}{\partial y}, \tag{8}$$

$$\frac{\partial C(y, \bar{t})}{\partial \bar{t}} = D_m \frac{\partial^2 C(y, \bar{t})}{\partial y^2}. \tag{9}$$

The appropriate initial and boundary conditions are

$$w(y, 0) = 0, \quad C(y, 0) = C_\infty, \quad T(y, 0) = T_\infty, \quad \frac{\partial w(y, 0)}{\partial \bar{t}} = 0, \quad y \geq 0, \tag{10}$$

$$C(0, \bar{t}) = C_w, \quad w(0, \bar{t}) = f_1(\bar{t}), \quad \frac{\partial T(0, \bar{t})}{\partial y} = -\frac{h}{k} T(0, \bar{t}). \tag{11}$$

where

$$f_1(\bar{t}) = \begin{cases} u_0 \frac{\bar{t}}{t_0}, & 0 < \bar{t} \leq t_0; \\ u_0, & \bar{t} > t_0 \end{cases}, \tag{12}$$

$$\bar{t} \geq 0: \quad w(y, \bar{t}) \rightarrow 0, \quad C(y, \bar{t}) \rightarrow \infty, \quad T(y, \bar{t}) \rightarrow \infty \quad \text{as } y \rightarrow \infty. \tag{13}$$

Some new dimensionless variables are introducing as:

$$\begin{aligned} t^* &= \frac{\nu h^2}{k^2} \bar{t}, & y^* &= \frac{h}{k} y, & w^* &= \frac{w}{u_0}, & \theta &= \frac{T(y, \bar{t}) - T_\infty}{T_\infty}, & \psi &= \frac{C(y, \bar{t}) - C_\infty}{C_\infty}, \\ P_r &= \frac{\mu C_p}{k}, & G_r &= \frac{g\beta_T T_\infty}{\nu u_0} \left(\frac{k}{h}\right)^2, & N_r &= \frac{16\sigma_1 T_\infty^3}{3kK_1}, & G_m &= \frac{g\beta_C C_\infty}{\nu u_0} \left(\frac{k}{h}\right)^2, \\ M &= \frac{k^2 \sigma \beta_0^2}{h^2 \nu}, & \lambda_2^* &= \frac{\nu h^2}{k^2} \lambda_2, & Sc &= \frac{\nu}{D_m}, & Pr_0 &= \frac{P_r}{1 + N_r}, & S &= \frac{k}{h} \frac{\mathbb{S}}{u_0 \mu}. \end{aligned} \tag{14}$$

and removing the star notation the required dimensionless equations are:

$$\frac{\partial w(y, t)}{\partial t} = \frac{1}{1 + \lambda_1} \left( 1 + \lambda_2 \frac{\partial}{\partial t} \right) \frac{\partial^2 w(y, t)}{\partial y^2} + Gr\theta(y, t) + Gm\psi(y, t) - Mw(y, t), \tag{15}$$

$$Pr_0 \frac{\partial \theta(y, t)}{\partial t} = \frac{\partial^2 \theta(y, t)}{\partial y^2}, \tag{16}$$

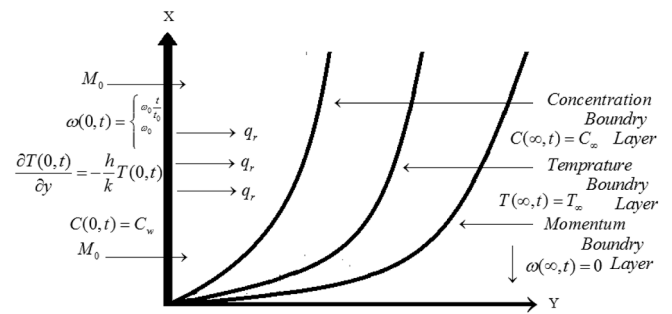


Fig. 1. Geometrical formation of the flow model.

$$(1 + \lambda_1)S = \left( 1 + \lambda_2 \frac{\partial}{\partial t} \right) \frac{\partial w(y, t)}{\partial y}, \tag{17}$$

$$\frac{\partial \psi(y, t)}{\partial t} = \frac{1}{Sc} \frac{\partial^2 \psi(y, t)}{\partial y^2}. \tag{18}$$

and corresponding set of initial and boundary conditions are:

$$w(y, 0) = 0, \quad \theta(y, 0) = 0, \quad \psi(y, 0) = 0, \tag{19}$$

$$w(0, t) = \begin{cases} t, & 0 < t \leq 1, \\ 1, & t > 1, \end{cases} \quad \frac{\partial \theta(0, t)}{\partial y} = -(1 + \theta(0, t)), \quad \psi(0, t) = 1, \tag{20}$$

$$w(y, t) \rightarrow 0, \quad \theta(y, t) \rightarrow 0, \quad \psi(y, t) \rightarrow 0, \quad \text{as } y \rightarrow \infty \quad \text{and } t \geq 0. \tag{21}$$

### Preliminaries

By definition the Fractional time derivative for Caputo-Fabrizio (CF) is mentioned as:

$${}^c FD_t^\varphi f(y, t^\sim) = \frac{1}{1 - \varphi} \int_0^{t^\sim} \exp\left(-\frac{\varphi(t^\sim - \tau)}{1 - \varphi}\right) \frac{\partial f(y, \tau)}{\partial \tau} d\tau, \quad 0 < \varphi < 1. \tag{22}$$

and its Laplace transform is obtained as:

$$\mathcal{L}\left({}^c FD_t^\varphi f(y, t^\sim)\right) = \frac{\nu \mathcal{L}\left(f(y, t^\sim)\right) - f(y, 0)}{(1 - \varphi)\nu + \varphi}. \tag{23}$$

where  $\varphi$  is a fractional parameter and  $\nu$  is Laplace parameter (Fig. 1).

### Solution of the problem

#### Exact solution of heat profile

Applying the definition provided in Eq. (22) for CF on Eq. (16) and plugging Eqs. (19)–(21) yield.

$${}^c FD_t^\varphi \theta(y, t) = \frac{1}{Pr_0} \frac{\partial^2 \theta(y, t)}{\partial y^2}, \tag{24}$$

Above equation becomes after employing Laplace transformation

$$\frac{\partial^2 \bar{\theta}(y, s)}{\partial y^2} - Pr_0 \left( \frac{s}{(1 - \alpha)s + \alpha} \right) \bar{\theta}(y, s) = 0. \tag{25}$$

with

$$\frac{\partial \bar{\theta}(0, s)}{\partial y} + \bar{\theta}(0, s) + \frac{1}{s} = 0, \quad \bar{\theta}(y, s) \rightarrow 0 \quad \text{as } y \rightarrow \infty. \tag{26}$$

By using Eq. (26), the Eq. (25) has the solution in the form:

$$\begin{aligned} \bar{\theta}(y, s) &= -\frac{e^{-y\sqrt{\frac{bPr_0s}{s+c}}}}{s(1-\sqrt{\frac{bPr_0s}{s+c}})}, \\ &= -\bar{\theta}_1(y, s) \cdot \left[ \frac{1}{a} + \left(\frac{ac-c}{a}\right)\bar{\theta}_2(y, s) + \left(\frac{\sqrt{bPr_0}}{a}\right)\bar{\theta}_3(y, s) \right]. \end{aligned} \tag{27}$$

After applying inverse laplace transformation on Eq. (27), the solution is

$$\theta(y, t) = -\left(\frac{1}{a}\right)\theta_1(y, t) + \left(\frac{c-ac}{a}\right)(\theta_1 * \theta_2)(t) - \left(\frac{\sqrt{bPr_0}}{a}\right)(\theta_1 * \theta_3)(t). \tag{28}$$

where

$$\begin{aligned} \theta_1(y, t) &= \mathcal{L}^{-1}\{\bar{\theta}_1(y, s)\} = \mathcal{L}^{-1}\left\{\frac{e^{-y\sqrt{\frac{Pr_0s}{(1-\alpha)s+\alpha}}}}{s}\right\}, \\ &= 1 - \frac{2Pr_0}{\pi} \int_0^{\infty} \frac{\sin\left(\frac{y}{\sqrt{1-\alpha}}\chi\right)}{\chi(Pr_0 + \chi^2)} e^{-\left(\frac{\alpha}{1-\alpha}\right)t\chi^2} d\chi, \\ \theta_2(y, t) &= \mathcal{L}^{-1}\{\bar{\theta}_2(y, s)\} = \mathcal{L}^{-1}\left\{\frac{1}{s+\frac{c}{a}}\right\} = e^{-\frac{c}{a}t}, \\ \theta_3(y, t) &= \mathcal{L}^{-1}\{\bar{\theta}_3(y, s)\} = (\theta_4 * \theta_5)(t), \\ \theta_4(y, t) &= \mathcal{L}^{-1}\{\bar{\theta}_4(y, s)\} = \mathcal{L}^{-1}\{\sqrt{s}\} = -\frac{1}{2\sqrt{\pi t^3}}, \\ \theta_5(y, t) &= \mathcal{L}^{-1}\{\bar{\theta}_5(y, s)\} = \mathcal{L}^{-1}\left\{\frac{\sqrt{s+c}}{s+\frac{c}{a}}\right\} \\ &= \frac{e^{-ct}}{\sqrt{\pi t}} + \sqrt{c-\frac{c}{a}} e^{-\frac{c}{a}t} \operatorname{erf}\left(\sqrt{c-\frac{c}{a}}t\right), b = \frac{1}{1-\alpha}, \quad c = ba \quad \text{and} \quad a \\ &= 1 - bPr_0. \end{aligned} \tag{29}$$

**Exact solution of mass profile**

Applying the definition provided in Eq. (22) for CF on Eq. (18) and plugging Eqs. (19)–(21) yield.

$${}^cFD_t^\alpha \psi(y, t) = \left(\frac{1}{S_c}\right) \frac{\partial^2 \psi(y, t)}{\partial y^2}. \tag{30}$$

Above equation becomes after employing Laplace transformation

$$\frac{\partial^2 \bar{\psi}(y, s)}{\partial y^2} - S_c \left(\frac{s}{(1-\alpha)s+\alpha}\right) \bar{\psi}(y, s) = 0. \tag{31}$$

with

$$\bar{\psi}(0, s) = \frac{1}{s}, \quad \bar{\psi}(y, s) \rightarrow 0 \quad \text{as} \quad y \rightarrow \infty. \tag{32}$$

By using Eq. (32), the Eq. (31) has the solution in the form:

$$\bar{w}(y, s) = \left(\frac{1-e^{-s}}{s^2}\right) e^{-y\sqrt{\frac{(b_1s+c_1)}{(b_3s+c_2)}}} - \frac{G_r(s+c)^2 \left( e^{-y\sqrt{\frac{(b_1s+c_1)}{(b_3s+c_2)}}} - e^{-y\sqrt{\frac{bPr_0s}{s+c}}} \right)}{s(1-\sqrt{\frac{bPr_0s}{s+c}})[(b_3s+c_2)bPr_0s - (b_1s+c_1)(s+c)]} + \frac{G_m(s+c)^2 \left( e^{-y\sqrt{\frac{(b_1s+c_1)}{(b_3s+c_2)}}} - e^{-y\sqrt{\frac{bPr_0s}{s+c}}} \right)}{s[(b_3s+c_2)bS_c s - (b_1s+c_1)(s+c)]}. \tag{39}$$

$$\bar{w}(y, s) = \left(\frac{1}{s}\right) e^{-y\sqrt{\frac{S_c s}{(1-\alpha)s+\alpha}}}. \tag{33}$$

Employing Inverse Laplace Transformation, the exact solution for concentration is written as:

$$\begin{aligned} \psi(y, t) &= L^{-1} \left( \frac{e^{-y\sqrt{\frac{S_c s}{(1-\alpha)s+\alpha}}}}{s} \right), \\ &= 1 - \frac{2S_c}{\pi} \int_0^{\infty} \frac{\sin\left(\frac{y}{\sqrt{1-\alpha}}\chi\right)}{\chi(S_c + \chi^2)} e^{-\left(\frac{\alpha}{1-\alpha}\right)t\chi^2} d\chi. \end{aligned} \tag{34}$$

**Nusselt number**

Nusselt number, which is used to estimate the rate of heat transfer can be obtained as:

$$Nu = -\frac{\partial \theta(y, t)}{\partial y} \Big|_{y=0} \tag{35}$$

**Exact solution of velocity profile**

Applying the definition provided in Eq. (22) for CF time fractional operator on Eq. (15) which gives

$$\begin{aligned} {}^cFD_t^\alpha w(y, t) &= \frac{1}{1+\lambda_1} \left( 1 \right. \\ &\quad \left. + \lambda_2 {}^cFD_t^\alpha \right) \frac{\partial^2 w(y, t)}{\partial y^2} + Gr\theta(y, t) + Gm\psi(y, t) - Mw(y, t), \end{aligned} \tag{36}$$

Employing Laplace transformation on the above equation

$$\begin{aligned} \left(\frac{s}{(1-\alpha)s+\alpha}\right) \bar{w}(y, s) &= \frac{1}{1+\lambda_1} \left( 1 + \lambda_2 \frac{s}{(1-\alpha)s+\alpha} \right) \frac{\partial^2 \bar{w}(y, s)}{\partial y^2} + G_r \bar{\theta}(y, s) \\ &\quad + G_m \bar{\psi}(y, s) - M \bar{w}(y, s), \\ \left(M + \frac{bs}{s+c}\right) \bar{w}(y, s) &= a_1 \left( 1 + \frac{\lambda_2 bs}{s+c} \right) \frac{\partial^2 \bar{w}(y, s)}{\partial y^2} + G_r \bar{\theta}(y, s) + G_m \bar{\psi}(y, s), \\ \left(\frac{b_1s+c_1}{s+c}\right) \bar{w}(y, s) &= a_1 \left(\frac{b_2s+c}{s+c}\right) \frac{\partial^2 \bar{w}(y, s)}{\partial y^2} + G_r \bar{\theta}(y, s) + G_m \bar{\psi}(y, s). \end{aligned} \tag{37}$$

from Eq. (27) and Eq. (33) substituting the values of  $\bar{\theta}(y, s)$  and  $\bar{\psi}(y, s)$ , the solution of Eq. (37) is written as

$$\begin{aligned} \bar{w}(y, s) &= A e^{y\sqrt{\frac{(b_1s+c_1)}{(b_3s+c_2)}}} + B e^{-y\sqrt{\frac{(b_1s+c_1)}{(b_3s+c_2)}}} \\ &\quad + \frac{G_r(s+c)^2 e^{-y\sqrt{\frac{bPr_0s}{s+c}}}}{s(1-\sqrt{\frac{bPr_0s}{s+c}})[(b_3s+c_2)bPr_0s - (b_1s+c_1)(s+c)]} \\ &\quad + \frac{G_m(s+c)^2 e^{-y\sqrt{\frac{bPr_0s}{s+c}}}}{s[(b_3s+c_2)bS_c s - (b_1s+c_1)(s+c)]}. \end{aligned} \tag{38}$$

To find the values of A, B, using initial/boundary conditions for velocity, the solution has the form

In Eq. (39) it is difficult to derive the exact solution due to involvement of complex combinations of terms. Consequently, the only efficient way to calculate exact result of the considered problem, write the Eq. (39) in series equivalent form then employing inverse Laplace transformation technique.

Eq. (39) can be arrange in the following way:

$$\begin{aligned} \bar{w}(y, s) &= \bar{\Psi}(y, s) - e^{-s}\bar{\Psi}(y, s) + G_r\bar{\Phi}(y, s)[\bar{\Omega}(y, s)\bar{\Pi}(y, s) \\ &\quad + \bar{\theta}(y, s)] + G_m\bar{\Theta}(y, s)[\bar{\Omega}(y, s) - \bar{\psi}(y, s)], \\ &= \bar{\Psi}(y, s) - e^{-s}\bar{\Psi}(y, s) + G_r\bar{\Phi}(y, s)[\bar{\Omega}(y, s) \\ &\quad + \bar{\theta}(y, s)] + G_m\bar{\Theta}(y, s)[\bar{\Omega}(y, s) - \bar{\psi}(y, s)]. \end{aligned} \tag{40}$$

Applying inverse Laplace transformation with convolution product on Eq. (40), we get the required solution

$$\begin{aligned} w(y, t) &= \Psi(y, t) - \Psi(y, \tau)H(\tau) + G_r[(\Phi^*\Omega)(t) + (\Phi^*\theta)(t)] + G_m[(\Theta^*\Omega)(t) \\ &\quad - (\Theta^*\psi)(t)]. \end{aligned} \tag{41}$$

where  $H(\tau)$  represent a standard Heaviside function with  $\tau = t - 1$  and

$$\begin{aligned} \Psi(y, t) &= \mathcal{L}^{-1}\left(\frac{e^{-y\sqrt{\frac{(b_1+s+c_1)}{(b_3+s+c_2)}}}}{s^2}\right), \\ &= \mathcal{L}^{-1}\left(\frac{e^{-y\sqrt{\frac{(p+2)}{(1+qz)}}}}{s^2}\right), \\ &= \frac{\gamma}{\epsilon} \int_0^\infty \int_0^t e^{-\frac{(p\gamma+z)}{c}} \operatorname{erfc}\left(\frac{y}{2\sqrt{z}}\right) I_0\left(\frac{2}{\epsilon}\sqrt{(\gamma-\eta\epsilon)pz}\right) dz dp \\ &\quad + \frac{\eta}{\epsilon} \int_0^\infty \int_0^t \int_0^t e^{-\frac{(p(1+\eta)+z)}{c}} \operatorname{erfc}\left(\frac{y}{2\sqrt{z}}\right) I_0\left(\frac{2}{\epsilon}\sqrt{(\gamma-\eta\epsilon)qp}\right) dz dq dp, \\ \bar{\Pi}(y, s) &= \mathcal{L}^{-1}\left(\frac{1}{1-\sqrt{\frac{bPr_0}{s+c}}}\right), \\ &= \mathcal{L}^{-1}\left(\frac{1}{a}\right) + \mathcal{L}^{-1}\left(\left(\frac{ac-c}{a}\bar{\theta}_2(y, s) + \left(\frac{\sqrt{bPr_0}}{a}\bar{\theta}_3(y, s)\right)\right)\right), \\ &= \mathcal{L}^{-1}\left(\frac{1}{a}\right) + \bar{\Pi}_1(y, s) \end{aligned} \tag{42}$$

$$\bar{\Pi}_1(y, s) = \mathcal{L}^{-1}\left(\left(\frac{ac-c}{a}\bar{\theta}_2(y, s) + \left(\frac{\sqrt{bPr_0}}{a}\bar{\theta}_3(y, s)\right)\right)\right),$$

$$\Pi_1(y, t) = \frac{(ac-c)}{a}\theta_2(y, t) + \left(\frac{\sqrt{bPr_0}}{a}\theta_3(y, t)\right),$$

$$\theta_2(y, t) = \mathcal{L}^{-1}\{\bar{\theta}_2(y, s)\} = \mathcal{L}^{-1}\left\{\frac{1}{s+\frac{c}{a}}\right\} = e^{-\frac{c}{a}t},$$

$$\theta_3(y, t) = \mathcal{L}^{-1}\{\bar{\theta}_3(y, s)\} = (\theta_4^*\theta_5)(t),$$

$$\theta_4(y, t) = \mathcal{L}^{-1}\{\bar{\theta}_4(y, s)\} = \mathcal{L}^{-1}\{\sqrt{s}\} = -\frac{1}{2\sqrt{\pi t^3}},$$

$$\theta_5(y, t) = \mathcal{L}^{-1}\{\bar{\theta}_5(y, s)\} = \mathcal{L}^{-1}\left\{\frac{\sqrt{s+c}}{s+\frac{c}{a}}\right\} = \frac{e^{-ct}}{\sqrt{\pi t}} + \sqrt{c-\frac{c}{a}}e^{-\frac{c}{a}t} \operatorname{erf}\left(\sqrt{c-\frac{c}{a}}t\right),$$

$$\Omega(y, t) = \mathcal{L}^{-1}\left(\frac{e^{-y\sqrt{\frac{(b_1+s+c_1)}{(b_3+s+c_2)}}}}{s}\right),$$

$$= \mathcal{L}^{-1}\left(\frac{e^{-y\sqrt{\frac{(p+2)}{(1+qz)}}}}{s}\right),$$

$$= e^{-y\sqrt{\eta}} - \frac{y\sqrt{\gamma}}{2\pi} \int_0^\infty \int_0^t \frac{1}{\sqrt{t}} e^{-(\epsilon t + \frac{z}{4\epsilon} + \eta v)} I_1(2\sqrt{\gamma v t}) dt dv,$$

$$\Omega(y, t) = \mathcal{L}^{-1}\{\bar{\Omega}(y, s)\} = \mathcal{L}^{-1}\left\{\frac{1}{a}\bar{\Omega}(y, s) + \bar{\Omega}(y, s)\bar{\Pi}_1(y, s)\right\} = \frac{1}{a}\Omega(y, t) + (\Omega^*\Pi_1)(t),$$

$$\bar{\Phi}(y, s) = \frac{(s+c)^2}{b_4s^2 + b_5s + c_3},$$

$$= \sum_{l=0}^\infty \sum_{\delta=0}^\infty \frac{(-1)^l l! (b_4)^{l-\delta} (b_5)^\delta}{(\delta)!(l-\delta)!(c_3)^{1+l}} \cdot \frac{1}{s^{\delta-2l-2}}$$

$$+ \sum_{l=0}^\infty \sum_{\delta=0}^\infty \frac{2c(-1)^l l! (b_4)^{l-\delta} (b_5)^\delta}{(\delta)!(l-\delta)!(c_3)^{1+l}} \cdot \frac{1}{s^{\delta-2l-1}}$$

$$+ \sum_{l=0}^\infty \sum_{\delta=0}^\infty \frac{(-1)^l l! c^2 (b_4)^{l-\delta} (b_5)^\delta}{(\delta)!(l-\delta)!(c_3)^{1+l}} \cdot \frac{1}{s^{\delta-2l}}$$

$$\Phi(y, t) = \sum_{l=0}^\infty \sum_{\delta=0}^\infty \frac{(-1)^l l! (b_4)^{l-\delta} (b_5)^\delta}{(\delta)!(l-\delta)!(c_3)^{1+l}} \cdot \frac{t^{\delta-2l-3}}{\Gamma(\delta-2l-2)}$$

$$+ \sum_{l=0}^\infty \sum_{\delta=0}^\infty \frac{2c(-1)^l l! (b_4)^{l-\delta} (b_5)^\delta}{(\delta)!(l-\delta)!(c_3)^{1+l}} \cdot \frac{t^{\delta-2l-2}}{\Gamma(\delta-2l-1)}$$

$$+ \sum_{l=0}^\infty \sum_{\delta=0}^\infty \frac{(-1)^l l! c^2 (b_4)^{l-\delta} (b_5)^\delta}{(\delta)!(l-\delta)!(c_3)^{1+l}} \cdot \frac{t^{\delta-2l-1}}{\Gamma(\delta-2l)}$$

$$\bar{\Theta}(y, s) = \frac{(s+c)^2}{b_6s^2 + b_7s + c_3}$$

$$= \sum_{l_1=0}^\infty \sum_{\delta_1=0}^\infty \frac{(-1)^{l_1} l_1! (b_6)^{l_1-\delta_1} (b_7)^{\delta_1}}{(\delta_1)!(l_1-\delta_1)!(c_3)^{1+l_1}} \cdot \frac{1}{s^{\delta_1-2l_1-2}}$$

$$+ \sum_{l_1=0}^\infty \sum_{\delta_1=0}^\infty \frac{2c(-1)^{l_1} l_1! (b_6)^{l_1-\delta_1} (b_7)^{\delta_1}}{(\delta_1)!(l_1-\delta_1)!(c_3)^{1+l_1}} \cdot \frac{1}{s^{\delta_1-2l_1-1}}$$

$$+ \sum_{l_1=0}^\infty \sum_{\delta_1=0}^\infty \frac{(-1)^{l_1} l_1! c^2 (b_6)^{l_1-\delta_1} (b_7)^{\delta_1}}{(\delta_1)!(l_1-\delta_1)!(c_3)^{1+l_1}} \cdot \frac{1}{s^{\delta_1-2l_1}}$$

$$\Theta(y, t) = \sum_{l_1=0}^\infty \sum_{\delta_1=0}^\infty \frac{(-1)^{l_1} l_1! (b_6)^{l_1-\delta_1} (b_7)^{\delta_1}}{(\delta_1)!(l_1-\delta_1)!(c_3)^{1+l_1}} \cdot \frac{t^{\delta_1-2l_1-3}}{\Gamma(\delta_1-2l_1-2)}$$

$$+ \sum_{l_1=0}^\infty \sum_{\delta_1=0}^\infty \frac{2c(-1)^{l_1} l_1! (b_6)^{l_1-\delta_1} (b_7)^{\delta_1}}{(\delta_1)!(l_1-\delta_1)!(c_3)^{1+l_1}} \cdot \frac{t^{\delta_1-2l_1-2}}{\Gamma(\delta_1-2l_1-1)}$$

$$+ \sum_{l_1=0}^\infty \sum_{\delta_1=0}^\infty \frac{(-1)^{l_1} l_1! c^2 (b_6)^{l_1-\delta_1} (b_7)^{\delta_1}}{(\delta_1)!(l_1-\delta_1)!(c_3)^{1+l_1}} \cdot \frac{t^{\delta_1-2l_1-1}}{\Gamma(\delta_1-2l_1)}$$

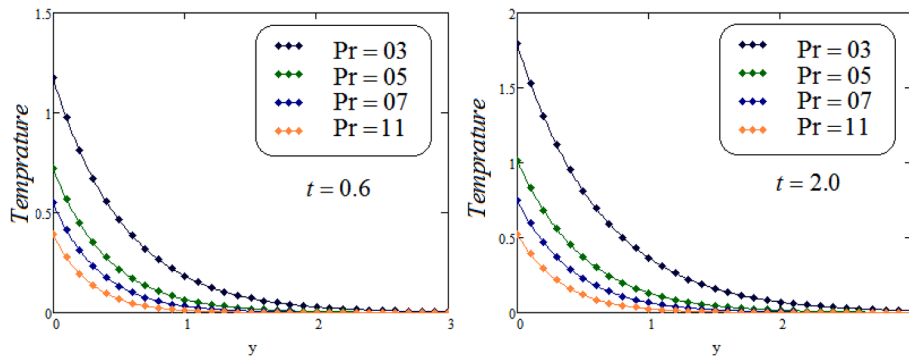


Fig. 2. Temperature profile for different  $Pr$  values at two different time levels  $t = 0.6$  and  $t = 2.0$ .

$$a = 1 - bPr_0, \quad a_1 = \frac{1}{1 + \lambda_1}, \quad b = \frac{1}{1 - \alpha}, \quad c = b\alpha, \quad c_1 = Mc, \quad c_2 = a_1c, \quad c_3 = -cc_1,$$

$$b_1 = M + b, \quad b_2 = 1 + \lambda_2b, \quad b_3 = a_1b_2, \quad b_4 = b_3bPr_0 - b_1, \quad b_5 = bPr_0c_2 - b_1c - c_1,$$

$$b_6 = b_3bS_c - b_1, \quad b_7 = bS_c c_2 - b_1c - c_1, \quad \gamma = \frac{b_1}{c_2}, \quad \eta = \frac{c_1}{c_2}, \quad \epsilon = \frac{b_3}{c_2}.$$

**Limiting cases**

We recover the same Jeffery fluid model graphically in the absence of mass grashof number, i.e,  $G_m = 0$  as obtained by Talha Anwar et al. [43].

The velocity distribution for integral order of Jeffery model is attained by applying the limit  $\alpha \rightarrow 1$  in Eq. (39) is written as:

tial parameters such as  $Pr, G_r, G_m$ , fractional parameter  $\alpha$ , time relaxation parameter  $\lambda_1$ , time retardation parameter  $\lambda_2, S_c$  and  $M$  on energy, concentration and velocity profile. It is realized that the fractional parameter  $\alpha$  controls the temperature, concentration, and velocity profiles. Figure 2 is portrayed the effect of  $Pr$ , on heat profile for two different time levels. It is noticed that thermic layer and temperature decreases by greater values of  $Pr$ . As  $Pr$  increase, the heat profile reduce more quickly. Actually, for insignificant values of  $Pr$ , thermic conductivity elevate which permits heat to defuse away quickly for increasing values of  $Pr$ .

Figs. 3 and 4 illustrated the effect of fractional parameter  $\alpha$  and time on temperature. It is detected that increasing the values of time which elevate the temperature distribution in Fig. 3. It is observed from Fig. 4 the behavior of temperature is decreasing for increasing the value of

$$\bar{w}(y, s) = \left( \frac{1 - e^{-s}}{s^2} \right) e^{-y\sqrt{\frac{s+M}{a_1(1+\lambda_2s)}}} - \frac{G_r \left( e^{-y\sqrt{\frac{s+M}{a_1(1+\lambda_2s)}}} - e^{-y\sqrt{Pr_0s}} \right)}{a_1s(1 - \sqrt{Pr_0s})[(1 + \lambda_2s)Pr_0s - (s + M)]} + \frac{G_m \left( e^{-y\sqrt{\frac{s+M}{a_1(1+\lambda_2s)}}} - e^{-y\sqrt{S_c s}} \right)}{a_1s[(1 + \lambda_2s)S_c s - (s + M)]}. \tag{43}$$

Furthermore, the solution of velocity distribution of second grade fluid is derived by implementing  $\lambda_1 \rightarrow 0$  in Eq. (39) and written as:

fractional parameter.

Also Fig. 5 illustrates the behavior of concentration for  $S_c$  at two different values of time, it is depicted that concentration is decreasing as the value of  $S_c$  is increasing. Figs. 6 and 7 displays the concentration is

$$\bar{w}(y, s) = \left( \frac{1 - e^{-s}}{s^2} \right) e^{-y\sqrt{\frac{(b_1s+c_1)}{(b_2s+c)}}} - \frac{G_r(s+c)^2 \left( e^{-y\sqrt{\frac{(b_1s+c_1)}{(b_2s+c)}}} - e^{-y\sqrt{\frac{bPr_0s}{s+c}}} \right)}{s(1 - \sqrt{\frac{bPr_0s}{s+c}})[(b_2s+c)bPr_0s - (b_1s+c_1)(s+c)]} + \frac{G_m(s+c)^2 \left( e^{-y\sqrt{\frac{(b_1s+c_1)}{(b_2s+c)}}} - e^{-y\sqrt{\frac{bS_c s}{s+c}}} \right)}{s[(b_2s+c)bS_c s - (b_1s+c_1)(s+c)]}. \tag{44}$$

This indicates the compatibility of our derived result with the literature.

**Results and discussion**

This section is dedicated to presenting the physical explanation of the exact results from CF fractional model obtained by Laplace transformation, as well as exploring the effects of flow parameters on the temperature, concentration and velocity of the Jeffery fluid. The graphical images are represented to examine the influences of substan-

increasing for growing values of fractional parameter  $\alpha$  and time. Furthermore, in Figs. 4 and 7, it is noticed that when  $\alpha \rightarrow 1$ , the CF fractional order model approaches to integer order model. Fig. 8 illustrates the behavior of prandtl number. Velocity is a decreasing function of  $Pr$ . Relevant heat and conductivity are both influenced by  $Pr$ . The thickness of the momentum and boundary layer is controlled by  $Pr$ .

Fig. 9 described the impact on  $G_r$  for velocity field. It has been found that as  $G_r$  increases, so does the velocity. In a physical sense for large values of  $G_r$ , the fluid flow rises due to the thermic buoyancy effects. The effect of  $G_m$  on jeffery fluid flow is displayed in Fig. 10. It has been perceived that the velocity field lifted corresponding to greater values of



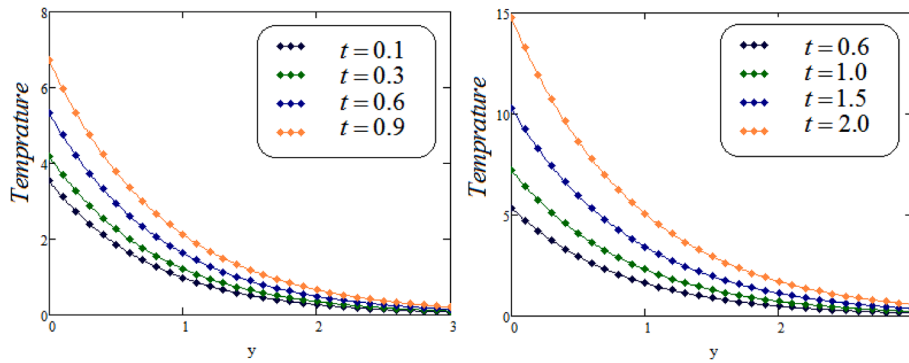


Fig. 3. Temperature profile for various  $t$  values for  $Pr = 1.2$  and  $\alpha = 0.3$ .

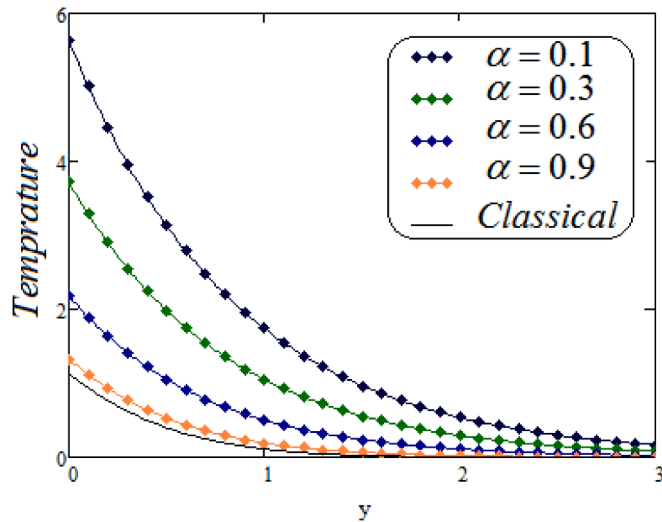


Fig. 4. Temperature association with varying values of  $\alpha$  with  $t = 0.4$  and  $Pr = 1.3$ .

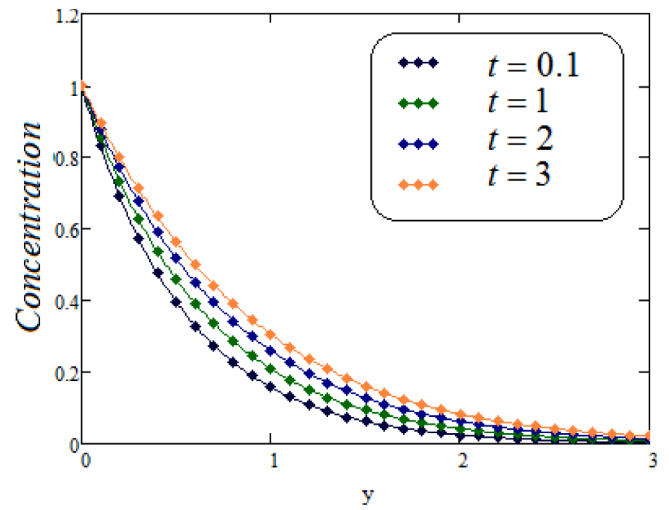


Fig. 6. Concentration profile for varying  $t$  values for  $\alpha = 0.3$  and  $Sc = 2.5$ .

$G_m$ . It is true that when  $G_m$  has large values then the buoyancy forces which weaken the viscous forces and fluid velocity accelerated.

In Fig. 11 influence of  $M$  is discussed on velocity profile. It is examine that decay in ramped velocity when increase in magnetic field. In Figs. 12 and 13, it is examined the impact of time relaxation parameter  $\lambda_1$  and time retardation parameter  $\lambda_2$  on velocity profile. For greater value of  $\lambda_1$ , the velocity and the boundary layer thickness reduced. This is for the reason that a slower regaining process is analyzed for the higher relaxation time, which causes the boundary layer thickness raised at a slower rate. When the values of  $\lambda_2$  increased which leads to enlarge the fluid velocity and boundary layer thickness also. It is analyzed that velocity shows opposite behavior for time relaxation parameter  $\lambda_1$  and

time retardation parameter  $\lambda_2$ . Fig. 14 depicts the influence of  $Sc$  on ramped velocity. It is observed that for higher values of  $Sc$  causes the retardation in the velocity. The matter behind that  $Sc$  is the ratio of viscous forces to mass diffusion, so higher values of  $Sc$  provided that stability to the viscous forces and dimness to the mass diffusion which produces decay in ramped velocity.

It is observed that the variation of fractional parameter  $\alpha$  on the fluid velocity profile and comparison between Talha Anwar et al. [43] with the considered problem in the absence of mass Grashof number and the CF fractional model with an ordinary model are discussed in figures Figs. 15 and 16. The velocity profile reduced by enlarging the value of fractional parameter  $\alpha$ . Fig. 17 shows that the velocity of the jeffrey fluid increases as  $t$  increases. Finally, it is noticed that when  $\alpha \rightarrow 1$ , the CF

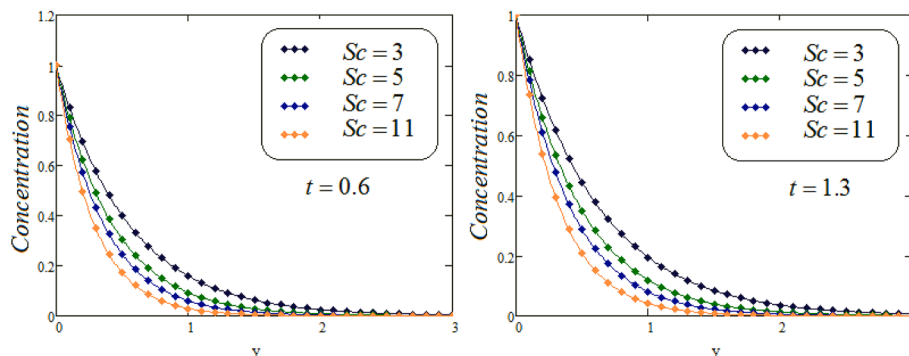


Fig. 5. Concentration profile for varying values of  $Sc$  for two different time levels  $t = 0.6$  and  $t = 1.3$ .

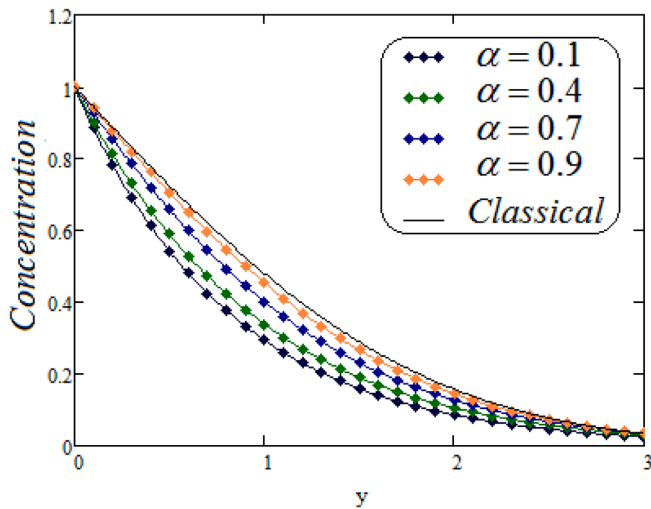


Fig. 7. Concentration association with varying values of  $\alpha$  with  $t = 1.6$  and  $S_c = 1.6$ .

fractional model becomes ordinary model as shown in Figs. 16 and 15 displayed the same graph as Talha Anwar et al. [43] when  $Gm = 0$  in our results.

**Conclusion**

In the present paper, the MHD convective flow of Jeffrey fluid model is studied. The governing differential equation is written into a dimensionless form subject to the application of CF time fractional operator. Exact solutions are derived via Laplace transformation technique for temperature, concentration and velocity. Also discussed distinct parameters via graphically to analyzed their effects on ramped velocity, concentration and Newtonian heating. Some significant remarks and concluding results are given below: • It has been established that decay in concentration and temperature for increasing the values of  $S_c$  and  $P_r$  respectively. • It is noticed that concentration and temperature profile are elevated for higher values of time  $t$ . • It is confirmed that the relaxation time parameter  $\lambda_1$  and retardation time parameter  $\lambda_2$  increases then fluid velocity decreases and increases respectively. • It is analyzed that the decay in temperature and velocity but increase in

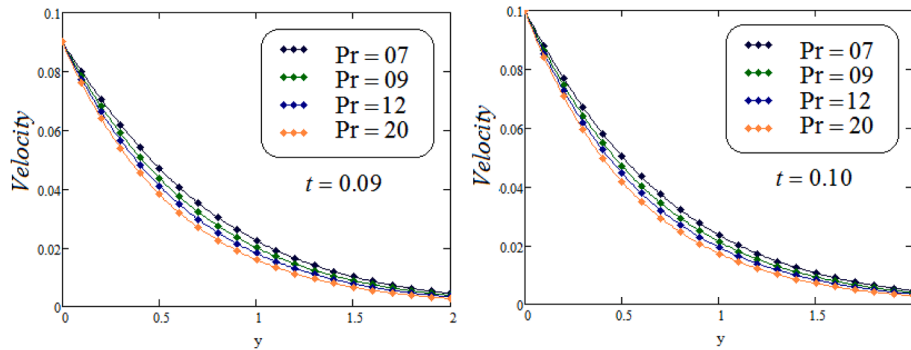


Fig. 8. Velocity profile for various  $Pr$  values at two different time levels  $t = 0.09$  and  $t = 0.10$  when  $M = 1.1, \alpha = 0.8, Gr = 0.25, Gm = 3.5, \lambda_1 = 1.2, \lambda_2 = 0.5, S_c = 1.2$ .

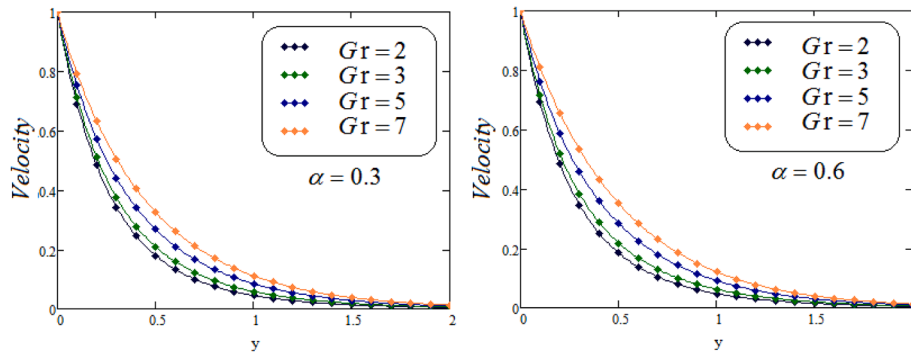


Fig. 9. Velocity for varying values of  $Gr$  when  $M = 1.1, Pr = 9, Gm = 3.5, \lambda_1 = 1.2, \lambda_2 = 0.5, S_c = 1.2$ .

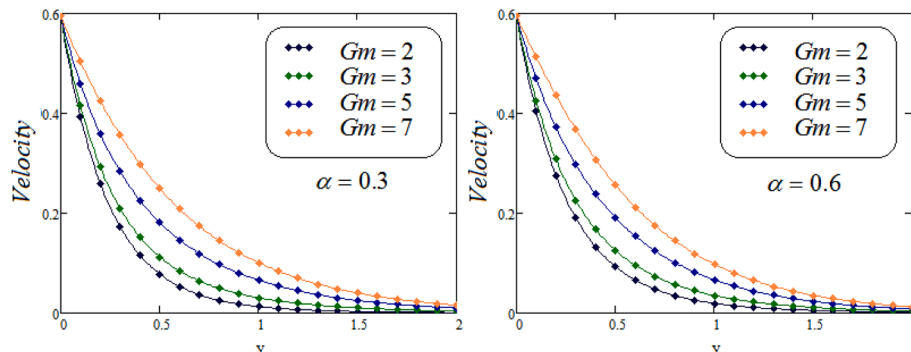


Fig. 10. Velocity for varying values of  $G_m$  when  $M = 9, Pr = 9, t = 0.6, Gr = 5, \lambda_1 = 1.2, \lambda_2 = 0.5, S_c = 3$ .



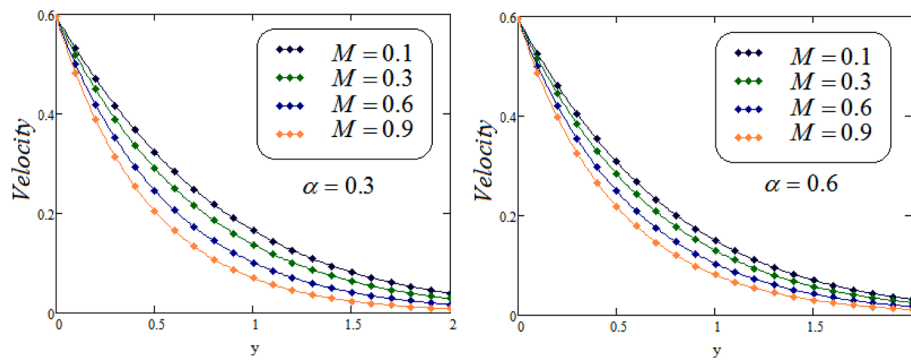


Fig. 11. Velocity for different values of  $M$  when  $Gm = 3.5, Pr = 9, t = 0.6, Gr = 0.25, \lambda_1 = 1.6, \lambda_2 = 0.5, Sc = 3$ .

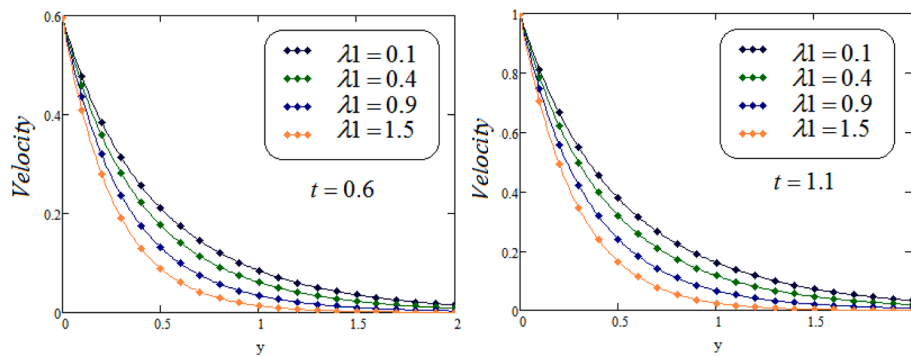


Fig. 12. Velocity for varying values of  $\lambda_1$  when  $Gm = 0.25, Pr = 9, t = 0.6, Gr = 5, M = 1.2, \lambda_2 = 0.1, Sc = 3, \alpha = 0.7$ .

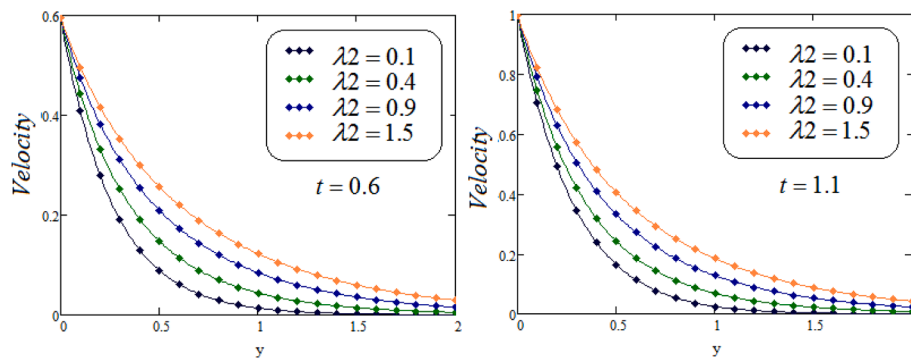


Fig. 13. Velocity for varying values of  $\lambda_2$  when  $Gm = 0.25, Pr = 9, t = 0.6, Gr = 5, M = 1.2, \alpha = 0.7, \lambda_1 = 1.5, Sc = 3$ .

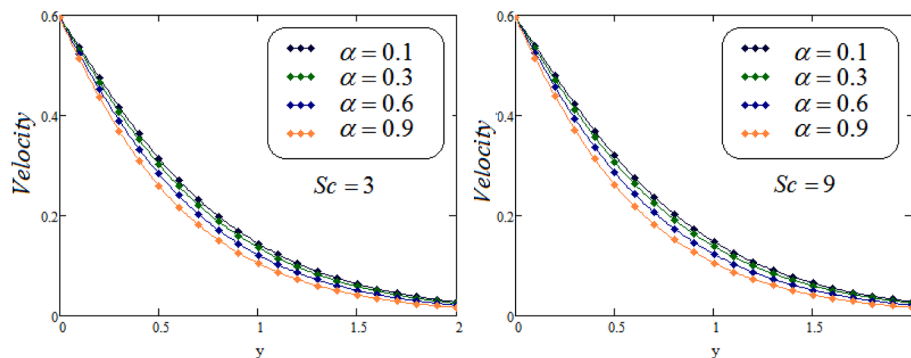


Fig. 14. Velocity for varying values of  $Sc$  when  $Gm = 0.25, Pr = 12, t = 0.6, Gr = 5, \lambda_1 = 0.5, \lambda_2 = 0.3, M = 1.5$ .

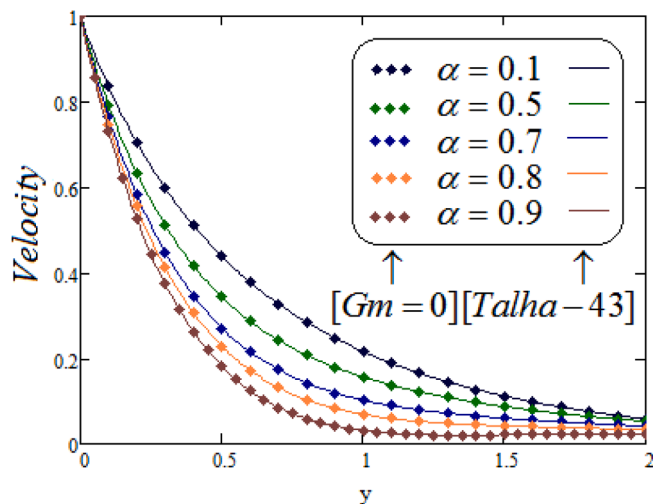


Fig. 15. Velocity comparison for varying values of  $\alpha$  when  $P_r = 12, Gr = 6, \lambda_1 = 0.5, \lambda_2 = 0.3, S_c = 15, M = 0.6$ .

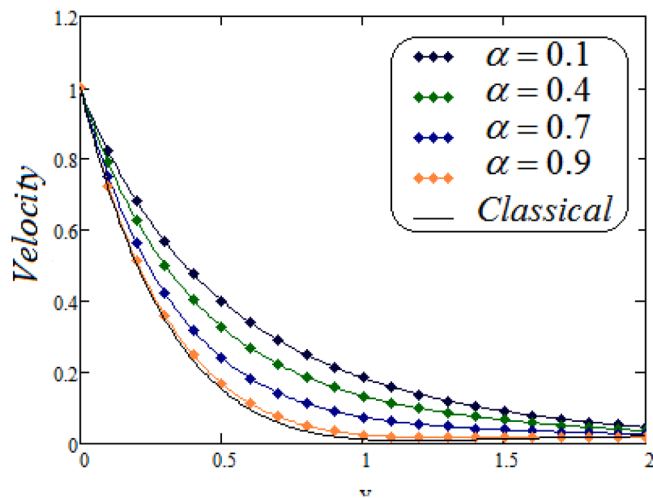


Fig. 16. Velocity for varying values of  $\alpha$  when  $Gm = 0.25, P_r = 12, Gr = 6, \lambda_1 = 0.5, \lambda_2 = 0.3, S_c = 15, M = 0.6$ .

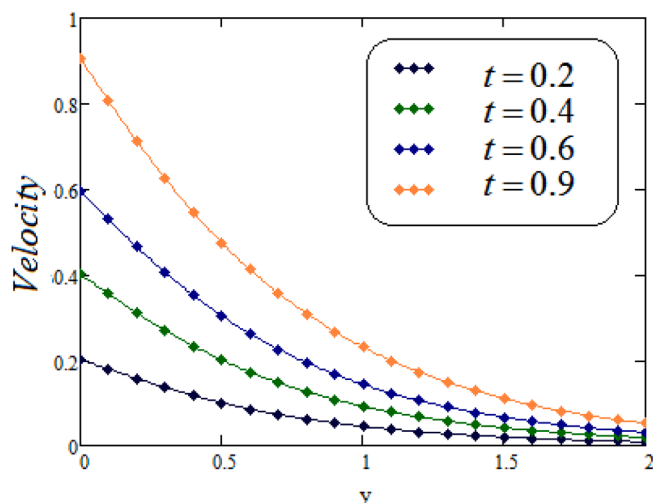


Fig. 17. Velocity profile for varying values of  $t$  when  $Gm = 0.25, P_r = 15, Gr = 5, \alpha = 0.7, \lambda_1 = 0.5, \lambda_2 = 0.3, S_c = 3, M = 0.6$ .

concentration for large values of fractional parameter  $\alpha$ . • The fluid velocity reduced when the values of  $M, S_c$  and  $P_r$  are increased. • For higher values of  $G_r$  and  $G_m$  the fluid velocity is increasing. • CF time fractional model converges to ordinary integer order model when  $\alpha \rightarrow 1$ .

#### Data availability

All the conformant material is accessible.

#### Authors' contributions

This article was written with fair and important contributions from all authors. The final manuscript was read and accepted by all contributors.

#### CRedit authorship contribution statement

**Aziz-Ur-Rehman:** Validation, Writing - review & editing. **Muhammad Bilal Riaz:** Conceptualization, Investigation, Methodology. **Jan Awrejcewicz:** Data curation, Project administration. **Dumitru Baleanu:** Software, Visualization, Supervision, Formal analysis.

#### Declaration of Competing Interest

The authors declare that they have no known competing financial interests or personal relationships that could have appeared to influence the work reported in this paper.

#### Acknowledgement

aaaa

#### References

- [1] Nadeem S, Mehmood R, Akbar NS. Non-orthogonal stagnation point flow of a nano non-Newtonian fluid towards a stretching surface with heat transfer. *Int J Heat Mass Transf* 2013;57:679–89.
- [2] Ghosh A, Sana P. On hydromagnetic flow of an Oldroyd-B fluid near a pulsating plate. *Acta Astronaut* 2009;64:272–80.
- [3] Kucuk F, Karakas M, Ayestaran L. Well testing and analysis techniques for layered reservoirs. *SPE Form Eval* 1986;1:342–54.
- [4] Mohyuddin MR, Hayat T, Mahomed F, Asghar S, Siddiqui AM. On solutions of some non-linear differential equations arising in Newtonian and non-Newtonian fluids. *Nonlinear Dyn* 2004;35:229–48.
- [5] Vajravelu K, Cannon J, Rollins D, Leto J. On solutions of some non-linear differential equations arising in third grade fluid flows. *Int J Eng Sci* 2002;40:1791–805.
- [6] Tasawar H, Ali N. Peristaltic motion of a jeffrey fluid under the effect of a magnetic field in a tube. *Commun Nonlinear Sci Numer Simul* 2008;13(7):1343–52.
- [7] Nadeem S, Akram S. Peristaltic flow of a jeffrey fluid in a rectangular duct. *Nonlinear Anal: Real World Appl* 2010;11(5):4238–47.
- [8] Nallapu S, Radhakrishnamacharya G. Jeffrey fluid flow through porous medium in the presence of magnetic field in narrow tubes. *Int J Eng Math* 2014.
- [9] Noor NFM. Analysis for MHD flow of a Maxwell fluid past a vertical stretching sheet in the presence of thermophoresis and chemical reaction. *World Acad Sci Technol* 2012;64:1019–23.
- [10] Jamil M, Fetecau C, Khan NA, Mahmood A. Some exact solutions for helical flows of Maxwell fluid in an annular pipe due to accelerated shear stresses. *Int J Chem React Eng* 2011;9.
- [11] Jamil M, Fetecau C, Fetecau C. Unsteady flow of viscoelastic fluid between two cylinders using fractional Maxwell model. *Acta Mech Sin* 2012;28:274–80.
- [12] Fetecau C, Fetecau C. The Rayleigh-Stokes-Problem for a fluid of Maxwellian type. *Int J Non-Linear Mech* 2003;38:603–7.
- [13] Filho Sobral. D.C.A new proposal to guide velocity and inclination in the ramp protocol for the treadmill ergometer. *Arq Bras De Cardiol* 2003;81:48–53.
- [14] Myers J, Bellin D. Ramp exercise protocols for clinical and cardiopulmonary exercise testing. *Sport Med* 2000;30:23–9.
- [15] Bruce R. Evaluation of functional capacity and exercise tolerance of cardiac patients. *Mod Concepts Cardiovasc Dis* 1956;25:321.
- [16] Kundu B. Exact analysis for propagation of heat in a biological tissue subject to different surface conditions for therapeutic applications. *Appl Math Comput* 2016; 285:204–16.
- [17] Malhotra CP, Mahajan RL, Sampath W, Barth KL, Enzenroth RA. Control of temperature uniformity during the manufacture of stable thin-film photovoltaic devices. *Int J Heat Mass Transf* 2006;49:2840–50.

- [18] Eichhorn R. Discussion: Free Convection From a Vertical Flat Plate With Step Discontinuities in Surface Temperature (Hayday, AA, Bowls, DA, and McGraw, RA, 1967. ASME J Heat Transfer 1967;89:244–249.
- [19] Schetz J. On the approximate solution of viscous-flow problems. J Appl Mech 1963;30:263–8.
- [20] Chandran P, Sacheti NC, Singh AK. Natural convection near a vertical plate with ramped wall temperature. Heat Mass Transf 2005;41:459–64.
- [21] Seth G, Ansari MS, Nandkeolyar R. MHD natural convection flow with radiative heat transfer past an impulsively moving plate with ramped wall temperature. Heat Mass Transf 2011;47:551–61.
- [22] Seth G, Hussain S, Sarkar S. Hydromagnetic natural convection flow with heat and mass transfer of a chemically reacting and heat absorbing fluid past an accelerated moving vertical plate with ramped temperature and ramped surface concentration through a porous medium. J Egypt Math Soc 2015;23:197–207.
- [23] Seth G, Sharma R, Sarkar S. Natural Convection Heat and Mass Transfer Flow with Hall Current, Rotation, Radiation and Heat Absorption Past an Accelerated Moving Vertical Plate with Ramped Temperature. J Appl Fluid Mech 2015;8:7–20.
- [24] Seth G, Sarkar S. MHD natural convection heat and mass transfer flow past a time dependent moving vertical plate with ramped temperature in a rotating medium with Hall effects, radiation and chemical reaction. J Mech 2015;31:91–104.
- [25] Seth G, Mahato G, Sarkar S. Effects of Hall current and rotation on MHD natural convection flow past an impulsively moving vertical plate with ramped temperature in the presence of thermal diffusion with heat absorption. Int J Energy Technol 2013;5:1–12.
- [26] Narahari M, Bég OA, Ghosh SK. Mathematical modelling of mass transfer and free convection current effects on unsteady viscous flow with ramped wall temperature. World J Mech 2011;1:176–84.
- [27] Khan. I.A note on exact solutions for the unsteady free convection flow of a Jeffrey fluid. Z Für Naturforschung A 2015;70:397–401.
- [28] Mohd Zin NA, Khan I, Shafie S. Influence of thermal radiation on unsteady MHD free convection flow of Jeffrey fluid over a vertical plate with ramped wall temperature. Math probl Eng 2016.
- [29] Ahmed N, Dutta M. Transient mass transfer flow past an impulsively started infinite vertical plate with ramped plate velocity and ramped temperature. Int J Phys Sci 2013;8:254–63.
- [30] Maqbool K, Mann A, Tiwana M. Unsteady MHD convective flow of a Jeffrey fluid embedded in a porous medium with ramped wall velocity and temperature. Alex Eng J 2018;57:1071–8.
- [31] Tiwana MH, Mann AB, Rizwan M, Maqbool K, Javeed S, Raza S, Khan MS. Unsteady Magnetohydrodynamic Convective Fluid Flow of Oldroyd-B Model Considering Ramped Wall Temperature and Ramped Wall Velocity. Mathematics 2019;7:676.
- [32] Saeed ST, Riaz MB, Baleanu D, Abro KA. A Mathematical Study of Natural Convection Flow Through a Channel with non-singular Kernels: An Application to Transport Phenomena. Alexandria Eng J 2020;59:2269–81.
- [33] Khan I, Saeed ST, Riaz MB, Abro KA, Husnine SM, Nissar KS. Influence in a Darcy's Medium with Heat Production and Radiation on MHD Convection Flow via Modern Fractional Approach. J Mater Res Technol 2020;9(5):10016–30.
- [34] Abro KA, Atangana A. Role of Non-integer and Integer Order Differentiations on the Relaxation Phenomena of Viscoelastic Fluid. Physica Scr 2020;95.
- [35] Atangana A, Baleanu D. New fractional derivative with non local and non-singular kernel: theory and application to heat transfer model. Therm Sci 2016;20:763–9.
- [36] Abro KA, Atangana A. A comparative study of convective fluid motion in rotating cavity via Atangana-Baleanu and Caputo-Fabrizio fractal-fractional differentiation. Eur Phys J Plus 135; 2020.
- [37] Riaz MB, Saeed ST, Baleanu D, Ghalib M. Computational results with non-singular and non-local kernel flow of viscous fluid in vertical permeable medium with variant temperature. Front Phys 2020;8:275.
- [38] Riaz MB, Saeed ST. Comprehensive analysis of integer order, Caputo-fabrizio and Atangana-Baleanu fractional time derivative for MHD Oldroyd-B fluid with slip effect and time dependent boundary condition. Discrete Continuous Dyn Syst 2020. <https://doi.org/10.3934/dcdss.2020.430>.
- [39] Imran MA, Aleem M, Riaz MB, Ali R, Khan I. A comprehensive report on convective flow of fractional (ABC) and (CF) MHD viscous fluid subject to generalized boundary conditions. Chaos Solitons Fractals 2018;118:274–89.
- [40] Riaz MB, Atangana A, Saeed ST. MHD free convection flow over a vertical plate with ramped wall temperature and chemical reaction in view of non-singular kernel. Wiley; 2020. p. 253–79.
- [41] Riaz MB, Atangana A, Iftikhar N. Heat and mass transfer in Maxwell fluid in view of local and non-local differential operators. J Therm Anal Calorim 2020.
- [42] Riaz MB, Iftikhar N. A comparative study of heat transfer analysis of MHD Maxwell fluid in view of local and non-local differential operators. Chaos Solitons Fractals 2020;132.
- [43] Anwar T, Kumam P, Asifa Khan I, Thounthong P. Generalized unsteady MHD Natural convective flow of Jeffrey Model with ramped wall velocity and Newtonian heating; a Caputo-Fabrizio Approach. C J Phys 2020. <https://doi.org/10.1016/cjph.2020.10.018>.
- [44] Khan M. Partial slip effects on the oscillatory flows of a fractional Jeffrey fluid in a porous medium. J Porous Media 2007;10(5):473–88.
- [45] Vanita V, Kumar A. Effect of radial magnetic field on free convective flow over ramped velocity moving vertical cylinder with ramped type temperature and concentration. J Appl Fluid Mech 2016;9(6):2855–64.
- [46] Martyushev SG, Sheremet MA. Characteristics of Rosseland and P-1 approximations in modeling nonstationary conditions of convection-radiation heat transfer in an enclosure with a local energy source. J Eng Thermophys 2012;21(2): 111–8.
- [47] A numerical investigation of Caputo time fractional Allen-Cahn equation using redefined cubic B-spline functions. Advances in Difference Eqs. 2020, 158.
- [48] A fourth order non-polynomial quintic spline collocation technique for solving time fractional superdiffusion equations, Advances in Differences Eqs. 2019, 514.
- [49] A numerical algorithm based on modified extended B-spline functions for solving time-fractional diffusion wave equation involving reaction and damping terms, Advances in Differences Equations, 2019, 378.